Pharmaceutical Sciences. 2025;31(4):403-412
doi:10.34172/PS.025.40930
https://ps.tbzmed.ac.ir/

Research Article

Lipid-Polymer Hybrid Chitosan-Stearic Acid Nanoparticles for Efficient Delivery of Berberine to Breast Cancer Cells

Elaheh-Sadat Saadatdar[1,2], Rafieh Bagherifar[2,3], Ali Rajabi Zangi[2,3], Atefeh Khodakarami[3,4], Roghaieh Holghoomi[5], Azita Dilmaghani[6*]

[1]Department of Chemical Engineering, Chemical Engineering Faculty, Sahand University of Technology, Tabriz, Iran
[2]Department of Pharmaceutics, Faculty of Pharmacy, Tabriz University of Medical Sciences, Tabriz, Iran
[3]Student Research Committee, Tabriz University of Medical Sciences, Tabriz, Iran
[4]Immunology Research Center, Tabriz University of Medical Sciences, Tabriz, Iran
[5]Department of Biology, Faculty of Sciences, Urmia University, Urmia, Iran
[6]Infectious and Tropical Diseases Research Center, Tabriz University of Medical Sciences, Tabriz, Iran

ARTICLE INFO

Article History:
Received: October 15, 2024
Revised: February 26, 2025
Accepted: March 16, 2025
ePublished: October 11, 2025

Keywords:
Berberine, Breast cancer, Chitosan, Hybrid nanoparticles, Stearic acid

Abstract

Background: Berberine (BBR) is a plant-derived isoquinoline alkaloid extensively studied for its anti-tumor properties. Despite its promising therapeutic potential, the clinical application of BBR has been significantly limited due to challenges such as poor aqueous solubility, suboptimal absorption, and low overall bioavailability. To address these issues, the encapsulation of BBR within nanoparticles (NPs) represents a promising strategy for improving its delivery and efficacy.

Methods: In this study, we developed novel lipid-polymer hybrid nanoparticles (LPHNPs) composed of chitosan (CS) and stearic acid (SA), specifically designed for the delivery of BBR to 4T1 breast cancer (BC) cells. The CS-SA NPs were synthesized through an oil-in-water emulsion/ionic gelation technique, optimizing their physicochemical properties for maximum drug encapsulation and release efficiency.

Results: The characterization of BBR-loaded CS-SA NPs (CS-SA/BBR NPs) revealed excellent physicochemical attributes, including favorable drug loading capacity and encapsulation efficiency, alongside a controlled release profile of BBR that was markedly slower than that of free BBR. In addition, CS-SA NPs displayed significantly higher in vitro cellular uptake in 4T1 cells. The cytotoxicity evaluation using the MTT assay demonstrated that the blank CS-SA NPs were non-toxic to the 4T1 cell line, indicating their biocompatibility. Additionally, *in ovo* assessment using the chick chorioallantoic membrane (CAM) assay revealed that CS-SA/BBR NPs significantly inhibited angiogenesis and reduced both the weight and size of tumors compared to treatment with free BBR.

Conclusion: Our findings suggest that CS-SA NPs constitute a novel and efficient drug delivery system (DDS) for BBR, enhancing its potential as a therapeutic agent in the management of BC. This encapsulation strategy not only improves the bioavailability of BBR but also minimizes its toxicity, paving the way for further investigations into its clinical application against BC and potentially other malignancies. Future studies should focus on evaluating the long-term efficacy and safety of this nanocarrier system in preclinical models as well as exploring its potential against different types of cancer cells.

Introduction

Berberine (BBR) is an isoquinoline alkaloid that is widely used as an antitumor, anti-inflammatory, immune modulator, and antioxidant agent due to its remarkable medicinal properties.[1,2] Recent studies have demonstrated that BBR could display potential antitumor effects by inhibiting the proliferation of cancer cells, inducing apoptosis and cell cycle arrest at G1/G0 phase in cancer cells.[3] Despite its therapeutic benefits, BBR is limited by its poor aqueous solubility, which leads to low bioavailability and insufficient absorption.[4] Additionally, the effect of the first-pass metabolism in both the liver and the intestine and its low permeability through the mucous layer of the intestine can also be considered as other reasons of low bioavailability.[5] Furthermore, the clinical application of BBR is limited due to its low stability and side effects associated with its intramuscular[6] and intravenous administration.[4,5,7] Recently, new strategies including nanoparticles (NPs) as drug delivery system (DDS), have been developed to overcome these challenges. The NP-mediated DDSs protect drugs from degradation and improve their therapeutic efficacy.[8]

Lipid-polymer hybrid NPs (LPHNPs), novel DDSs for improving the absorption of natural medicinal compounds,

***Corresponding Author:** Azita Dilmaghani, Email: dilmaghani.a@gmail.com

have recently been considered potential drug carriers.[9,10] LPHNPs typically consist of a lipid core surrounded by a polymer shell or vice versa. This combination provides the advantages of both lipids and polymers in terms of stability, drug loading capacity, and surface modifications. The lipid core can accommodate lipophilic drugs, whereas the polymer shell can encapsulate hydrophilic drugs, enabling the delivery of a broader range of therapeutic agents. The lipid core also provides structural integrity, while the polymer shell protects against degradation and aggregation. This improves the long-term stability of LPHNPs, making them less prone to drug leakage or particle aggregation.[11,12] LPHNPs are prepared using various methods, such as emulsion-evaporation, nanoprecipitation, or self-assembly techniques. These methods involve forming a stable core-shell structure by combining lipids and polymers in a controlled manner.[13]

Natural and biodegradable polymers, such as chitosan (CS), have demonstrated great prominence in encapsulating and delivering various anticancer drugs.[14] CS is a cationic polysaccharide with chemical modification potential and Food and Drug Administration-Generally Recognized as Safe (FDA-GRAS) status, allowing its application in the biotechnological and biomedical fields.[15] However, this polymer faces some challenges, such as high hydrophilicity, high molecular weight, and low drug loading capacity, which lead to problems in formulation.[16] In contrast, stearic acid (SA) is an endogenous and biocompatible fatty acid with low toxicity that can be combined with CS to yield a hybrid nanocarrier with the advantages of both agents.[17,18]

In this study, CS-SA/BBR NPs were prepared through an oil-in-water emulsion/ionic gelation method. These NPs have a core-shell structure in which SA core provides a space for efficient loading of hydrophobic BBR, while the hydrophilic CS shell protects the entrapped BBR and reduces its side effects. The physicochemical properties, release profile, and encapsulation efficiency (EE) of prepared NPs were investigated. Cellular uptake and cytotoxicity of NPs were assessed using flow cytometry and MTT assay, respectively. Finally, we developed a chick embryo chorioallantoic membrane (CAM) assay to evaluate the effect of CS-SA/BBR NPs on angiogenesis and tumor growth rate of 4T1 breast cancer (BC) cells.

Materials and Methods

CS (190-310 KDa and deacetylation 80%), SA, tripolyphosphate (TPP), Tween 80, and BBR were obtained from Sigma–Aldrich. All other analytical grade chemicals and solvents were also obtained from Merck Chemical Co.

Preparation of CS-SA/BBR NPs

CS-SA/BBR NPs were prepared using the oil-in-water emulsion/ionic gelation technique.[19] Briefly, CS was dissolved in a 2% v/v acetic acid solution (1 mg/mL) and stirred for 24 hours. Then, the pH of the solution was adjusted to 5 using NaOH (5 N), Tween 80 (1.2 mg/mL) was added, and the solution was placed in a water bath (50 ºC) for 2 hours. In the second step, SA (1 mg/mL) and BBR (0.16 mg/mL) were dissolved in ethanol and added dropwise to the CS solution under ultrasonication condition until the CS-SA/BBR NPs were formed through self-assembly. 2 mL TPP solution (0.1 mg/mL), as a crosslinking agent, was added to the emulsion under stirring, which was continued for another 20 min. Finally, the samples were lyophilized and stored until characterization. The composition of CS-SA/BBR NPs, including absolute quantities and percentages of key components.is summarized in Table 1.

Characterization of CS-SA/BBR NPs

Fourier-transform infrared spectroscopy (FT-IR) analysis

The chemical composition and structure of CS-SA/BBR NPs were investigated using an FT-IR spectrophotometer (BRUKER, Tensor 27) and KBr pellets with 32 scans at a resolution of 4 cm^{-1} over a wavenumber range of 4000–400 cm^{-1}.

X-ray diffraction (XRD) analysis

The crystalline structures of lyophilized powder samples were evaluated by XRD (Bruker AXS model D8). The XRD diffractograms were obtained at 2θ in the range of 2–50° using Cu K α radiation of the incident beam (λ = 1.5418 Å) at a voltage of 45 kV and a current of 0.8 mA. Moreover, the morphological features of NPs were visualized using scanning electron microscopy (SEM, Metropolitan-Vickers-UK).

Size distribution and zeta potential

The hydrodynamic diameter and polydispersity index (PDI) of the NPs were measured by dynamic light scattering (DLS) using a Malvern Instruments Ltd. (Malvern, UK). The freshly prepared CS-SA NPs with the concentration of 1 mg/mL at 25 °C were used for DLS analysis. Measurements were carried out using of disposable folded capillary cuvette, and before analysis, all the air bubbles were eliminated from the capillary. For decrease in opalescence, 1 mL of the NPs dispersion was diluted by distilled water in a 1:1 ratio before size measurement. Surface charge (zeta potential) was determined using the same instrument at 25 °C.

Drug loading (DL) and entrapment efficiency (EE)

DL and EE studies were carried out using UV-Vis spectroscopy (SHIMADZU UV-1800). 5 mg of CS-SA/BBR NPs were dispersed in 1 mL phosphate buffered saline (PBS), pH = 7.4, and centrifuged at 3000 rpm for 15 min using Amicon Ultra centrifugal filters, MWCO

Table 1. Composition of CS-SA/BBR NPs (quantities and percentages of total solids)

Component	BBR	CS	SA	TPP
Absolute quantity	8 mg	50 mg	50 mg	0.2 mg
Percentage	7.4 %	46.3 %	46.3 %	0.2 %

30 kDa. UV–visible spectrophotometry at 345 nm (λ_{max}) was used to determine the free drug concentration in the supernatant. The EE% and the DL% were calculated using the following equations[20]:

$$EE\% = \frac{Total\ drug\ weight - Free\ drug\ weight}{Total\ drug\ weight}$$

$$DL\% = \frac{Total\ drug\ weight - Free\ drug\ weight}{Total\ nanoparticles\ weight}$$

Biodegradation study

The in vitro degradation of CS-SA NPs in PBS was evaluated. About 2.8 mg (W_0) of CS-SA NPs were dispersed in 1x PBS (pH 6.5 and 7.4), and incubated at 37 °C for 12 days. After completion of the incubation period, the samples were centrifuged and washed with deionized water and freeze-dried. The dry weights of the samples were noted as Wt. The degradation rate was calculated by using the following formula:

$$Degradation\ rate(\%) = \frac{W0 - Wt}{W0}$$

Release study of BBR CS-SA/BBR NPs

In vitro release studies were performed using a dialysis bag.[21] Briefly, lyophilized CS-SA/BBR NPs were dispersed in 1 mL of PBS and poured into a cellulose dialysis bag (6-8 kDa, MWCO). Then, the dialysis bag was immersed in 50 mL of PBS (pH 7.4) and placed into a thermostatic shaking incubator at 37 °C and 120 rpm. A sample of 1 mL was withdrawn at different time intervals and replaced with an equivalent volume of fresh PBS. The amount of BBR released at each time interval was measured using UV/Vis spectroscopy (Shimadzu UV-1800) at 345 nm to plot the BBR release curve.

Plots of the kinetic models were made using Excel application to determine the kinetic model and mechanism of BBR release from the CS-SA NPs. The correlation coefficient (R^2) of highest degree establishes the kinetic model that best fits the release of BBR.[22]

Cell viability

The murine BC cell line (4T1) was obtained from the National Cell Bank of Pasteur Institute of Iran and cultured in RPMI 1640 medium (Gibco, Paisley, UK) supplemented with 10% fetal bovine serum (FBS), 100 U/mL penicillin and 100 U/mL streptomycin at 37 °C in 5% CO_2.

The MTT (3-[4,5-dimethylthiazol-2-yl]-2,5 diphenyl tetrazolium bromide) assay was used to determine cell viability.[23] Briefly, 4T1 cells (10^4 cells/well) were seeded into a 96-well plate and incubated for 24 hours. After 24 hours, when the confluence rate reached more than 70%, the cells were treated with different concentrations of BBR (0, 5, 10, 15, 20, 25, 30, 35 nM) to determine the IC50 value. To investigate the toxicity of blank or BBR-loaded NPs, 4T1 cells were also treated with CS-SA/BBR NPs and CS-SA NPs (BBR concentration equal to the IC50 value) and incubated at 37 °C in 5% CO_2 for 24 hours. After 24 hours, 20 µL of MTT solution (0.5 mg/mL) was added to each well, and the cells were incubated for 4 hours. Then, 150 µL DMSO was added to each well to dissolve the generated formazan crystals, and the plates were incubated until the solution process. After 30 minutes, the absorbance of the final solution was determined at two different wavelengths, 570 and 620 nm (background), using an ELISA (enzyme-linked immunosorbent assay) plate reader ($OD = OD_{570} - OD_{620}$).

Cellular uptake

4T1 cells were seeded on 6-well plates at a density of 5×10^5 cells/well. After 24 hours, the wells were treated with RD-B-loaded CS-SA NPs at a final concentration of 50 µg/mL and incubated at 37 °C for 4 hours. The free RD-B was removed by washing the wells with cold PBS. Then the cells were trypsinized and resuspended in 200 µL of PBS. Finally, the fluorescence intensity of the cells was determined using a flow cytometer (BD FACSCalibur, BD Biosciences, USA) and analyzed through FlowJo software (version 10).

Chick chorioallantoic membrane (CAM) assay

The CAM assay was used to study the effects of BBR and CS-SA/BBR NPs on angiogenesis and tumor growth rate.[24] Fertilized chicken eggs were incubated in a MultiQuip Incubator at 37 °C and 50%-60% humidity. On day 10 of chick embryo development, a small window (0.5 cm^2) was made in the egg shell under aseptic conditions, and the window was resealed with adhesive tape. The eggs were then returned to the incubator after injection of 10 µL of the 4T1 cell suspension containing $0.5–1 \times 10^6$ cells onto the CAM (n = 5) chicken embryos per free drug-treated cells, chicken embryos per CS-SA/BBR NPs treated cells and chicken embryos per untreated cells, considered as a control group). The 4T1 cells were treated for 24 hours before injection. The window was opened on day 17 of chick embryo development, and the tumor was removed. The effects of free drug and CS-SA/BBR NPs on the weight and size of the tumor and angiogenesis were investigated.

Statistical analysis

All assays were performed in triplicate. Data analyses were performed using GraphPad Prism, version 9.01. The results were analyzed using a one-way analysis of variance (ANOVA), followed by a post hoc test using Tukey's pairwise comparison assay. $P < 0.05$ was considered statistically significant.

Results

FT-IR analysis

Figure 1 demonstrates the FT-IR spectra of CS, SA, BBR, and CS-SA/BBR NPs. The characteristic peak related to NH_2 and OH stretching, which appeared at 3347 cm^{-1} in the CS spectra, has shifted to 3355 cm^{-1} and become narrower in the case of CS-SA NPs, indicating the

reduction of hydrogen bonding. The characteristic peaks of SA, including 2917 and 2848 cm^{-1} (aliphatic groups), 1700 cm^{-1} (C=O), and 1462 cm^{-1} (methylene groups) have also appeared in the CS-SA/BBR NPs spectra with a slight shift, which confirms the presence of SA in the structure of NPs. Moreover, new peaks around 1250-1100 cm^{-1} related to P-O and P=O could be attributed to the electrostatic interaction between phosphoric groups of TPP and ammonium ions of CS.

DLS study

The mean particle size and PDI were about 322±40.86 nm and 0.2, respectively (Figure 2).[25] The zeta potential of the NPs was+28 mV.

XRD pattern

XRD patterns of BBR, SA, CS, and CS-SA/BBR NPs are shown in Figure 3. XRD spectrum of pure SA exhibits several sharp diffraction peaks resulting from regular crystallization of SA. Additionally, sharp diffraction peaks in the XRD pattern of BBR indicates that BBR is crystalline.[26] The XRD pattern of CS displays broad lines with slighter diffraction angles and characteristic peaks of two points at 10° and 21° related to crystal forms I and II, respectively.[27] The peak observed in the diffractogram of the CS-SA/BBR NPs is broader compared to CS, which is probably due to the prevention of the formation of intramolecular and intermolecular hydrogen bonds in the structure of CS caused by the introduction of BBR and SA. Moreover, ultrasonication and cross-linking reactions

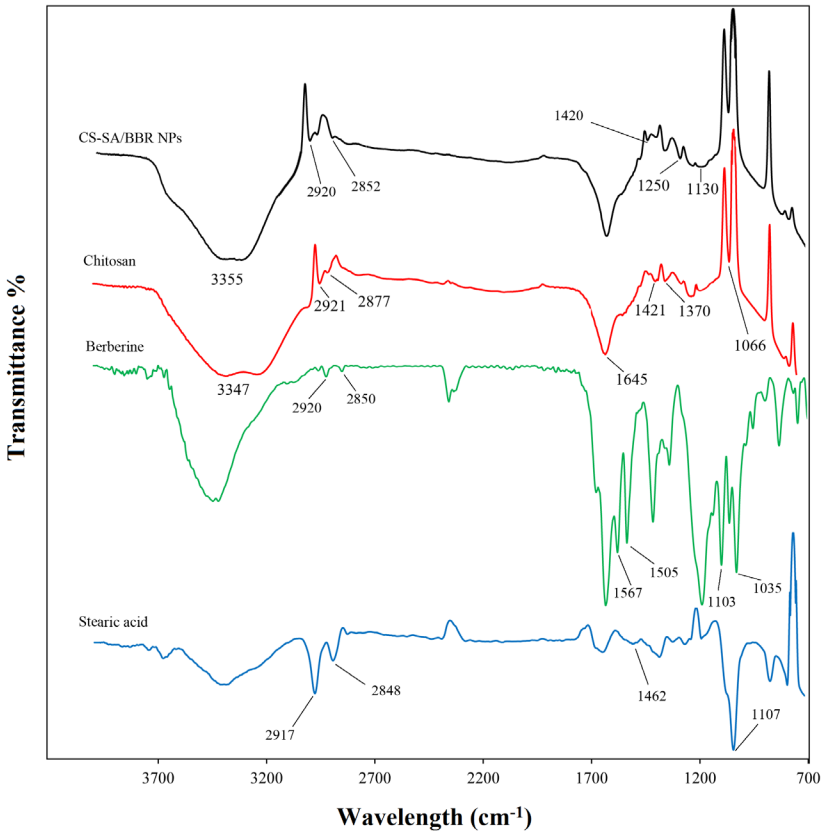

Figure 1. FT-IR spectra of CS, SA, BBR, and CS-SA/BBR NPs

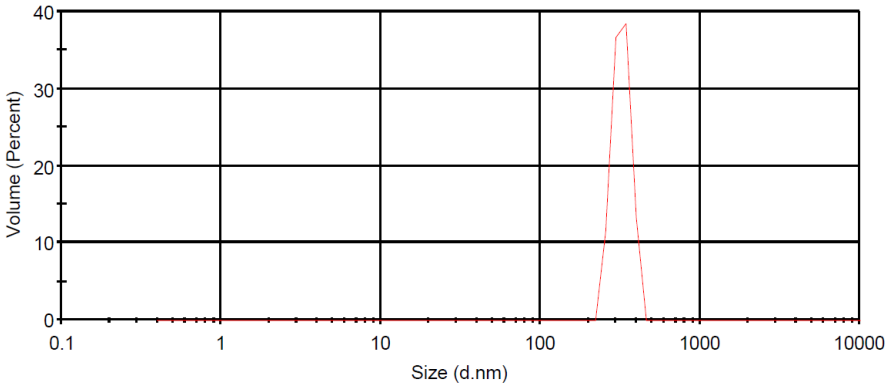

Figure 2. Particle size distribution of CS-SA/BBR NPs

between CS and TPP can cause disorganization in the polymer chains and destruction of the crystal structure of the nanocarrier, respectively.[28,29]

SEM analysis

SEM micrographs of the CS-SA/BBR NPs show a spherical shape without notable accumulation (Figure 4). Additionally, it demonstrates a homogeneous distribution of SA within the CS matrix.[30] As expected, the sizes of NPs (180-220 nm) were smaller than the hydrodynamic sizes determined by DLS, which can be attributed to the dehydration of the NPs during the sample preparation process for SEM.

Entrapment efficiency and drug loading

The EE and DL for CS-SA/BBR NPs were 71.25 ± 0.25% and 2.63 ± 0.03%, respectively. According to the amounts of EE and DL, it was observed that LPHNPs containing BBR have a high loading capacity and can help BBR to maintain its effective form, which indicates its proper and significant action during the absorption, distribution, metabolism and excretion in therapeutic applications.

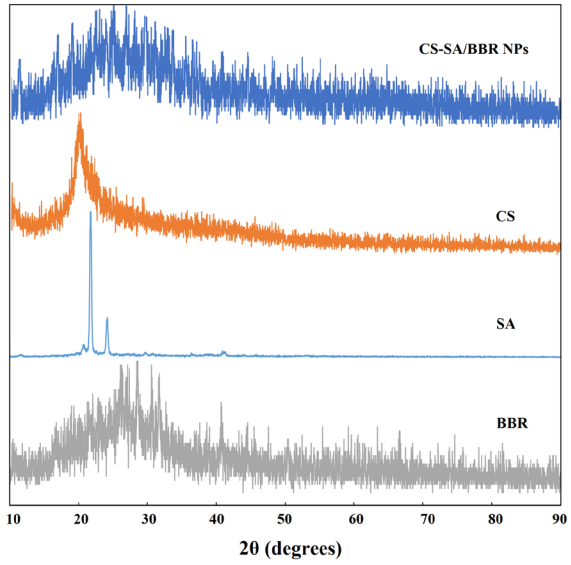

Figure 3. X-Ray diffraction patterns of BBR, CS, SA and CS-SA/BBR NPs

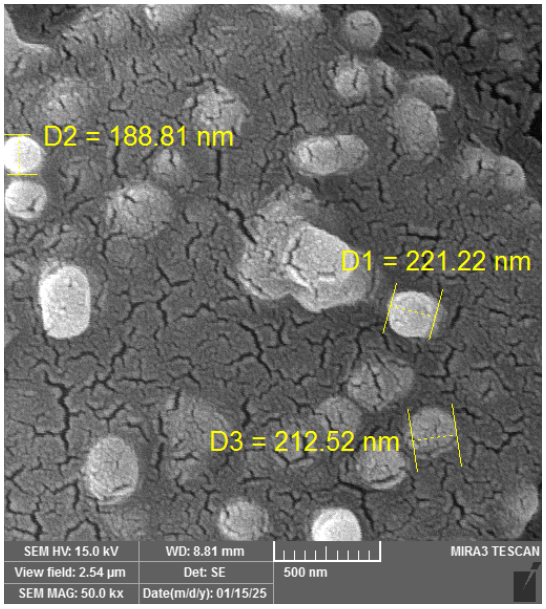

Figure 4. SEM image of CS-SA/BBR NPs

Biodegradation study

The rate of degradation after 12 days was 23% and 5% in PBS pH 6.5 and 7.4, respectively. As expected, the degradation rate in acidic media was significantly high in comparison to neutral pH.

Drug release

In vitro drug release profile of CS-SA/BBR NPs in PBS buffer (pH 7.4) for 72 hours is shown in Figure 5. A rapid release of BBR from CS-SA/BBR NPs (21.66%) occurred within the first 2 hours (burst effect), which may be attributed to the adsorption of BBR on the surface of NPs. After 2 hours, BBR was released slowly and with a low slope over 72 hours.[25] This is comparable to the release profile of free BBR solution, where the drug release occurred explosively and with a steep, so that more than 83% cumulative release was observed within 9 hours. Additionally, the cumulative release percentage in the case of free BBR and CS-SA/BBR NPs was about 69.6 and 98.66%, respectively. These results demonstrate that CS-SA/BBR NPs provide a continuous and sustained release of BBR compared to BBR solution, which indicates the ability of LPHNPs as a suitable carrier for therapeutic applications.

To determine the best kinetic model, linear regression with plots of the models was used. Table 2 shows that the Korsmeyer-Peppas model had the best fit, due to its highest R^2 value. The n and k parameters in the Korsmeyer-Peppas model were obtained from the slope (0.5) and intercept (1.75) of its respective plot, respectively. The slope of 0.5 indicates that drug release mechanism from the CS-SA NPs is non-Fickian diffusion. A non-Fickian drug release shows polymer relaxation/swelling controlled drug release.[31]

Cytotoxicity

The MTT assay was performed to determine the IC50 value of BBR, as well as the cytotoxic effect of CS-SA NPs and CS-SA/BBR NPs in 4T1 tumor cell line. The IC50 value was observed at 18.16 nM after 24 hours of treatment (Figure 6a). A constant concentration of 18.16

Table 2. Correlation coefficients for drug release kinetics

Kinetic models	Correlation coefficients (R^2)
Zero-order	0.62
First-order	0.75
Hixon-Crowell	0.71
Korsmeyer-Peppas	0.93
Higuchi	0.86

nM was used for BBR to compare the cytotoxic effect of NPs versus free BBR in the 4T1 cells. According to Figure 6b, no significant toxicity was observed for blank CS-SA NPs after 24 hours. This indicates that the NPs themselves are non-toxic to the cells. In contrast, CS-SA/BBR NPs demonstrated significantly higher cytotoxicity (73%) on 4T1 cells compared to free BBR (43.6%) and blank CS-SA NPs (6.96%). The results clearly show that CS-SA/BBR NPs inhibit 4T1 cell proliferation to a high extent, which can be due to the increase in BBR cellular uptake and the sustained release effect of CS-SA NPs.[32]

Cellular uptake

Cellular uptake of CS-SA NPs by 4T1 cells was studied via flow cytometry. The 2.2-fold higher mean fluorescence intensity (MFI) in CS-SA/RD-B NPs treated cells (218 vs. 98) indicates significantly greater fluorescence signal, directly correlating with higher uptake of NPs (Figure 7).

The effect of CS-SA/BBR NPs on angiogenesis and proliferation rate of 4T1 cells

The CAM assay is a widely used method to study angiogenesis as well as tumor growth rate. As shown in Figure 8, the angiogenesis rate in 4T1 cells treated with CS-SA/BBR NPs significantly decreased compared with free BBR and the control group (untreated group). Moreover, treatment with CS-SA/BBR NPs significantly reduced the weight and size of the tumors formed on the CAM layer, which could be attributed to the higher cellular uptake of NPs by 4T1 cells.

Discussion

BC is the most commonly diagnosed cancer worldwide Natural substances, such as BBR, are used to target specific treatments and offer a lower toxicity profile than traditional cancer treatments. BBR delivery to target tissues faces some challenges.[33] Nanoformulations such as LPHNPs are considered potential candidates for overcoming the limitations of BBR delivery due to their excellent benefits.[34,35] In the present study, CS-SA/BBR NPs were prepared and their effect on 4T1 cells was investigated. These NPs have a core-shell structure in which SA core provides a space for efficient loading of hydrophobic BBR, while the hydrophilic CS shell protects the entrapped BBR and reduces its side effects.[36]

The CS-SA/BBR NPs exhibited a nearly spherical morphology with a mean particle size of 322 ± 40.86 nm. The PDI value of 0.2 indicates a relatively narrow and

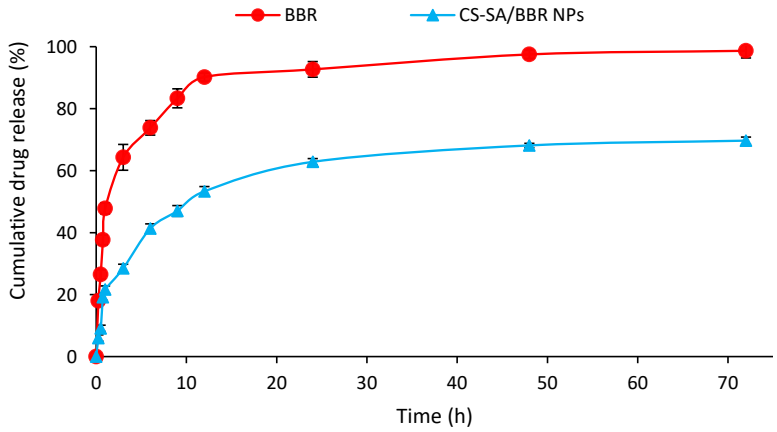

Figure 5. Cumulative release profiles of BBR solution and CS-SA/BBR NPs estimated by dialysis membrane method (mean ± SD; n = 3)

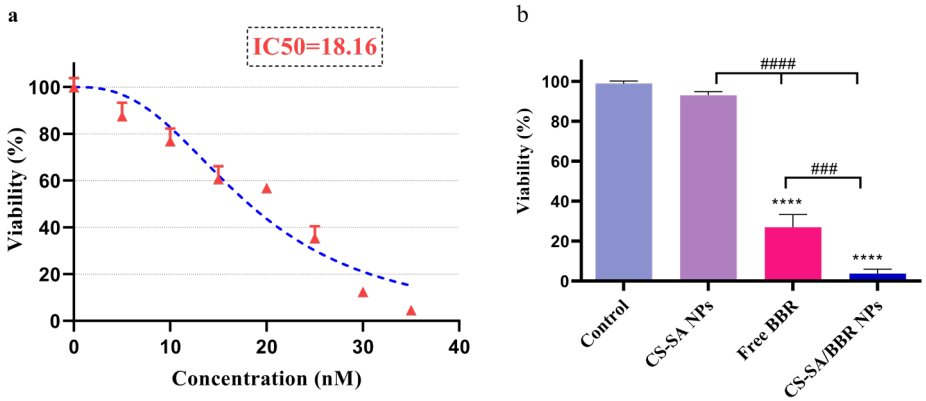

Figure 6. a) The IC50 value of BBR and b) the cytotoxicity of free BBR, blank CS-SA NPs, and CS-SA/BBR NPs on 4T1 cell line at 24 h. The data shown are representative of three independent experiments, which were presented as mean ± SD. SD: standard deviation. ****P < 0.0001 compared to the control group; ###P < 0.001 and ####P < 0.0001 compared to each treatment group

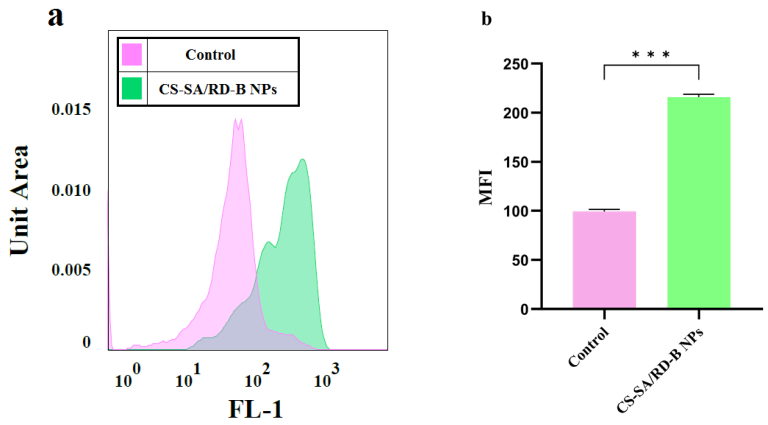

Figure 7. Cellular uptake of RD-B loaded CS-SA NPs after 4 h-incubation. a) Graphic demonstration of flowcytometry analysis of 4T1 cells, and b) Quantitative MFI histogram. The data shown are representative of three independent experiments, which were presented as mean ± SD. SD: standard deviation. ***P < 0.001 compared to the control group

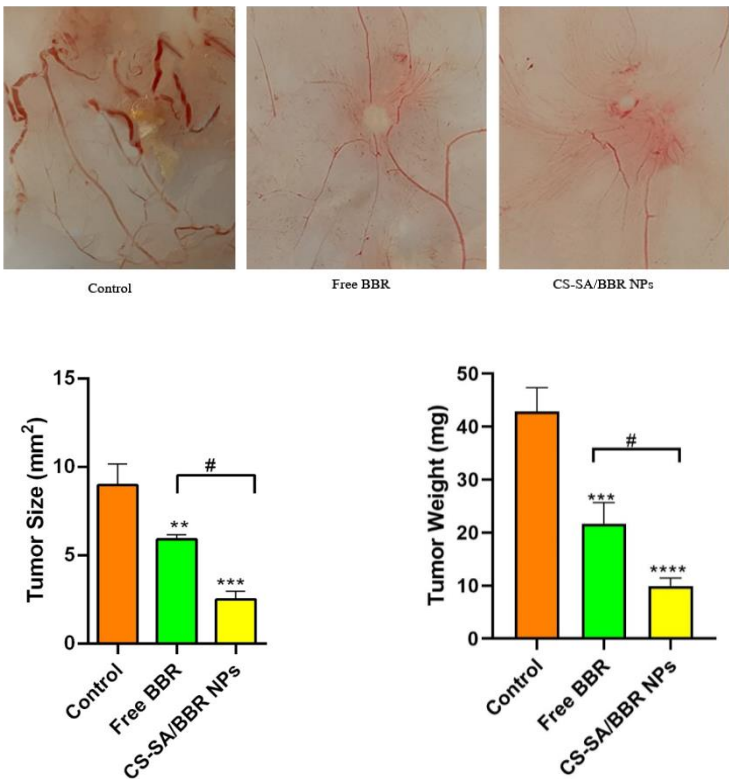

Figure 8. CAM assay was used to investigate the effect of free BBR and CS-SA/BBR NPs on the angiogenesis rate as well as the size and weight of the tumor. The data shown are representative of three independent experiments, which were presented as mean ± SD

uniform size distribution of the NPs, with most particles being of similar sizes. Moreover, the positive surface charge of + 28 mV confirms the presence of CS on the surface of the LPHNPs, attributed to the protonated amine groups in CS, and suggests that the NPs are suitable for achieving a stable formulation. Charged particles generally exhibit lower aggregation and higher stability compared to neutral particles.[37,38]

Biodegradation is a crucial process that influences the metabolic pathways of materials within the body, and it holds significant relevance for all NPs employed as DDSs. CS in the human body undergoes degradation through both chemical and enzymatic processes. CS is a polysaccharide composed of β-(1→4)-linked glucosamine and N-acetylglucosamine units. Its degradation in PBS 6.5 at 37 °C proceeds via hydrolysis of glycosidic bonds and conversion to soluble fragments, reducing NP mass, even at neutral pH, albeit slower than in acidic conditions. The degradation of CS was pH dependent as it is not soluble at physiological pH.[39,40] While, it seems that SA remains chemically stable *in vitro*, because Lipases (required for ester hydrolysis) are absent in PBS. As pH value of 7.4 and 6.5 represent the physiological pH and endosomal pH, respectively, these data indicated that CS-SA NPs would be remained stable in blood and be degraded after reaching to the target cells. The degradation results obtained in the

present study are in agreement with the one observed by Tomihata & Ikada and Saravanabhavan et al.[41,42]

The release study was performed in PBS (pH 7.4). BBR was initially released rapidly from the CS-SA/BBR NPs and then the drug release continued in a sustained manner for up to 72 hours.[43] The slow drug release shows that the core of the NPs remains intact and blocks the drug from being released in the physiological pH. Therefore, the bioactivity of the BBR is protected until the target is reached. Similarly, Gungor Ak et al, prepared BBR-CS NPs using ionotropic gelation method and investigated their release profile. The results showed that the release profile of BBR from the NPs was similar to our results.[25] In another study, BBR loaded LPHNPs containing CS as the polymer and nanostructured lipid carriers as the lipid shell were prepared. The authors demonstrated a biphasic drug release pattern, including a burst release within the first 1 h and a sustained release over 24 h, occurred from NPs.[44]

The cytotoxicity evaluation of BBR-loaded NPs and blank NPs by MTT method showed that blank NPs did not exhibit significant toxicity on 4T1 cells, and the high cytotoxicity observed for drug-loaded NPs compared to free BBR is only caused by BBR. CS-SA NPs may enhance cytotoxicity by improving cellular uptake of BBR through enhanced permeation and retention (EPR) effect owing to their small size. Additionally, the sustained release of BBR from the NPs could maintain prolonged exposure of 4T1 cells to the drug, exacerbating mitochondrial damage and apoptosis.[45] These data are consistent with cellular uptake results. Similarly, Jiang et al, prepared emodin-loaded LPHNPs comprising CS and SA and investigated their cytotoxic effect on MGC803 and BGC823 gastric cancer cells using MTT assay. The results demonstrated that CS-SA NPs are a safe delivery system with little biological toxicity.[21] In another study, redox-responsive CS-SA NPs are developed for co-delivery of doxorubicin (hydrophilic) and curcumin (hydrophobic) drugs to colorectal cancer cell line. The dual drug loaded CS-SA NPs demonstrated higher cytotoxicity against HCT116 cells. Blank NPs did not show significant toxicity.[46] Therefore, CS-SA NPs can be considered as a safe and nontoxic delivery system with good biocompatibility.

CS enhances cellular uptake via mucoadhesive properties and positive charge, promoting interaction with negatively charged cell membranes. Moreover, SA adds hydrophobicity, improving NPs stability and drug loading. This combination likely provides efficient endocytosis or membrane fusion.[47,48] In addition, CS-SA NPs accumulate in tumors through the EPR effect owing to their small size and the leaky and highly permeable nature of tumor vasculature. In a similar study, it was shown that after 4 hours incubation, the cellular uptake percentage of Chlorine e6 (Ce6) for CS-SA/Ce6 micelles by both A549 and HeLa cells was much more than that of the drug solution and remained unchanged after 4 hours (up to 24 hours), which might be due to the concentration-dependent cellular uptake of CS-SA/Ce6 micelles and Ce6 by tumor cells.[49] In another study, the authors demonstrated that FITC labeled CS-SA NPs have good cellular uptake activity and were distributed evenly in the cytoplasm of gastric cancer cells.[21]

The CAM assay is a relatively low-cost and straightforward method to evaluate angiogenesis, and it can be used to screen potential pro- or anti-angiogenic agents without causing any pain by the chick.[50] The CS-SA/BBR NPs inhibited angiogenesis significantly and very few larger vessels remained unaffected compared to the untreated group, which led to the inhibition of metastasis. Moreover, tumor size and weight decreased in the CS-SA/BBR NPs group compared to the free BBR and control group. These results are consistent with other literature reports on BBR encapsulated in various NPs. For example, Pund et al, prepared a self-nanoemulsifying drug delivery system (SNEDDS) of BBR and found that the formulation showed a potent anti-angiogenic effect compared to blank SNEDDS.[33] Similarly, in another study, a significant inhibition of angiogenesis was observed in human cervical cancer cells after BBR (10 μg) treatment when compared to DMSO-treated controls.[24] Furthermore, in another study, LPHNPs containing PEGylated lecithin-chitosan encapsulating alpha-terpineol were prepared, and their anti-angiogenic effects were investigated on MCF7 BC cells. The results demonstrated decreased angiogenesis and embryonic growth factors in CAM assay, as well as decreased expression of VEGF and VEGF-R genes, which is confirmed by qPCR, indicating the inhibitory effect of alpha-terpineol loaded LPHNPs on angiogenesis compared to free alpha-terpineol.[51]

In conclusion, CS-SA NPs can be used as a potential carrier to improve the antitumor activity of BBR.

Conclusion

Lipid NPs have garnered increasing attention in drug delivery, and CS, a cationic polysaccharide, has diverse applications in pharmaceutical sciences. In the present study, these two systems were combined to create LPHNPs, which offer significant advantages in drug delivery. BBR-loaded CS-SA hybrid NPs were successfully fabricated using the oil-in-water emulsion/ionic gelation method and characterized for various physicochemical parameters. The prepared formulation exhibited suitable particle size, EE%, DL%, and morphology. CS-SA/BBR NPs demonstrated a significantly slower release rate of BBR compared to free BBR. Moreover, the NPs displayed high cellular uptake in 4T1 cells. Cell viability studies confirmed the remarkable cytotoxic effect of BBR-loaded NPs on the 4T1 BC cell line over 24 hours. Furthermore, the CAM assay revealed that the CS-SA/BBR NPs significantly inhibited angiogenesis and tumor growth rate. It can be concluded that CS-SA NPs can be used as a potential carrier to improve the antitumor activity of BBR. Further studies in tumor animal models are necessary to

evaluate the effectiveness of LPHNPs.

Authors' Contribution

Conceptualization: Azita Dilmaghani.
Data curation: Azita Dilmaghani.
Methodology: Elaheh-Sadat Saadatdar, Rafieh Bagherifar.
Software: Atefeh Khodakarami.
Supervision: Azita Dilmaghani.
Validation: Azita Dilmaghani.
Writing–original draft: Elaheh-Sadat Saadatdar.
Writing–review & editing: Rafieh Bagherifar, Ali Rajabi Zangi, Roghaieh Holghoomi.

Competing Interests

The authors have no conflicts of interest to disclose.

Ethical Approval

This study was conducted on established cell lines and did not involve human participants or animal subjects; therefore, ethical committee approval and an ethical code were not required.

Funding

This research did not receive any any specific grant from funding agencies in the public, commercial or not-for-profit sectors.

References

1. Li AR, Zhu Y, Li XN, Tian XJ. Antimicrobial activity of four species of Berberidaceae. Fitoterapia. 2007;78(5):379-81. doi: 10.1016/j.fitote.2007.03.001.
2. Liu H, Li Y, Zhang X, Shi M, Li D, Wang Y. Chitosan-coated solid lipid nano-encapsulation improves the therapeutic anti-airway inflammation effect of berberine against COPD in cigarette smoke-exposed rats. Can Respir J. 2022;2022:8509396. doi: 10.1155/2022/8509396.
3. Wang L, Li H, Wang S, Liu R, Wu Z, Wang C, et al. Enhancing the antitumor activity of berberine hydrochloride by solid lipid nanoparticle encapsulation. AAPS PharmSciTech. 2014;15(4):834-44. doi: 10.1208/s12249-014-0112-0.
4. Xue M, Zhang L, Yang MX, Zhang W, Li XM, Ou ZM, et al. Berberine-loaded solid lipid nanoparticles are concentrated in the liver and ameliorate hepatosteatosis in db/db mice. Int J Nanomedicine. 2015;10:5049-57. doi: 10.2147/ijn.S84565.
5. Liu YT, Hao HP, Xie HG, Lai L, Wang Q, Liu CX, et al. Extensive intestinal first-pass elimination and predominant hepatic distribution of berberine explain its low plasma levels in rats. Drug Metab Dispos. 2010;38(10):1779-84. doi: 10.1124/dmd.110.033936.
6. Piroonpan T, Rimdusit P, Taechutrakul S, Pasanphan W. pH-responsive water-soluble chitosan amphiphilic core-shell nanoparticles: radiation-assisted green synthesis and drug-controlled release studies. Pharmaceutics. 2023;15(3):847. doi: 10.3390/pharmaceutics15030847.
7. Hua W, Ding L, Chen Y, Gong B, He J, Xu G. Determination of berberine in human plasma by liquid chromatography-electrospray ionization-mass spectrometry. J Pharm Biomed Anal. 2007;44(4):931-7. doi: 10.1016/j.jpba.2007.03.022.
8. Mujtaba MA, Akhter MH, Alam MS, Ali MD, Hussain A. An updated review on therapeutic potential and recent advances in drug delivery of berberine: current status and future prospect. Curr Pharm Biotechnol. 2022;23(1):60-71. doi: 10.2174/1389201022666210208152113.
9. Gajbhiye KR, Salve R, Narwade M, Sheikh A, Kesharwani P, Gajbhiye V. Lipid polymer hybrid nanoparticles: a custom-tailored next-generation approach for cancer therapeutics. Mol Cancer. 2023;22(1):160. doi: 10.1186/s12943-023-01849-0.
10. Xie Y, Gong X, Jin Z, Xu W, Zhao K. Curcumin encapsulation in self-assembled nanoparticles based on amphiphilic palmitic acid-grafted-quaternized chitosan with enhanced cytotoxic, antimicrobial and antioxidant properties. Int J Biol Macromol. 2022;222(Pt B):2855-67. doi: 10.1016/j.ijbiomac.2022.10.064.
11. Shah S, Famta P, Raghuvanshi RS, Singh SB, Srivastava S. Lipid polymer hybrid nanocarriers: Insights into synthesis aspects, characterization, release mechanisms, surface functionalization and potential implications. Colloid Interface Sci Commun. 2022;46:100570. doi: 10.1016/j.colcom.2021.100570.
12. Sengel-Turk CT, Paksoy AO, Alpturk O. The state of the art in core–shell-type lipid–polymer hybrid nanocarriers and beyond. Polym Bull. 2024;81(6):4771-800. doi: 10.1007/s00289-023-04951-x.
13. Sivadasan D, Sultan MH, Madkhali O, Almoshari Y, Thangavel N. Polymeric lipid hybrid nanoparticles (PLNs) as emerging drug delivery platform-a comprehensive review of their properties, preparation methods, and therapeutic applications. Pharmaceutics. 2021;13(8):1291. doi: 10.3390/pharmaceutics13081291.
14. Hezari S, Olad A, Dilmaghani A. Investigation of antibacterial properties and sustained release of *Centella asiatica* extract from Fe-MOF-reinforced gelatin-based hydrogels. Polym Bull. 2024;81(16):14701-25. doi: 10.1007/s00289-024-05416-5.
15. Wright L, Joyce P, Barnes TJ, Lundmark R, Bergström CA, Hubert M, et al. A comparison of chitosan, mesoporous silica and poly(lactic-co-glycolic) acid nanocarriers for optimising intestinal uptake of oral protein therapeutics. J Pharm Sci. 2021;110(1):217-27. doi: 10.1016/j.xphs.2020.09.026.
16. Hu FQ, Ren GF, Yuan H, Du YZ, Zeng S. Shell cross-linked stearic acid grafted chitosan oligosaccharide self-aggregated micelles for controlled release of paclitaxel. Colloids Surf B Biointerfaces. 2006;50(2):97-103. doi: 10.1016/j.colsurfb.2006.04.009.
17. Hu P, Wang T, Xu Q, Chang Y, Tu H, Zheng Y, et al. Genotoxicity evaluation of stearic acid grafted chitosan oligosaccharide nanomicelles. Mutat Res. 2013;751(2):116-26. doi: 10.1016/j.mrgentox.2012.12.004.
18. Atarian M, Rajaei A, Tabatabaei M, Mohsenifar A, Bodaghi H. Formulation of Pickering sunflower oil-in-water emulsion stabilized by chitosan-stearic acid nanogel and studying its oxidative stability. Carbohydr Polym. 2019;210:47-55. doi: 10.1016/j.carbpol.2019.01.008.
19. Motiei M, Kashanian S. Novel amphiphilic chitosan nanocarriers for sustained oral delivery of hydrophobic drugs. Eur J Pharm Sci. 2017;99:285-91. doi: 10.1016/j.ejps.2016.12.035.
20. Thotakura N, Dadarwal M, Kumar P, Sharma G, Guru SK, Bhushan S, et al. Chitosan-stearic acid based polymeric micelles for the effective delivery of tamoxifen: cytotoxic and pharmacokinetic evaluation. AAPS PharmSciTech. 2017;18(3):759-68. doi: 10.1208/s12249-016-0563-6.
21. Jiang X, Ma M, Li M, Shao S, Yuan H, Hu F, et al. Preparation and evaluation of novel emodin-loaded stearic acid-g-chitosan oligosaccharide nanomicelles. Nanoscale Res Lett. 2020;15(1):93. doi: 10.1186/s11671-020-03304-1 .
22. Ekenna IC, Abali SO. Comparison of the use of kinetic model plots and DD solver software to evaluate the drug release from griseofulvin tablets. J Drug Deliv Ther. 2022;12(2S):5-13. doi: 10.22270/jddt.v12i2-s.5402.
23. Khodakarami A, Afsari Kashani M, Nazer A, Mahmoudsalehi Kheshti A, Rashidi B, Karpisheh V, et al. Targeted silencing of NRF2 by rituximab-conjugated nanoparticles increases the sensitivity of chronic lymphoblastic leukemia cells to cyclophosphamide. Cell Commun Signal. 2023;21(1):188. doi: 10.1186/s12964-023-01213-1.
24. Chu SC, Yu CC, Hsu LS, Chen KS, Su MY, Chen PN. Berberine reverses epithelial-to-mesenchymal transition and inhibits metastasis and tumor-induced angiogenesis in human cervical cancer cells. Mol Pharmacol. 2014;86(6):609-23. doi:

10.1124/mol.114.094037 .
25. Gungor Ak A, Turan I, Sayan Ozacmak H, Karatas A. Chitosan nanoparticles as promising tool for berberine delivery: formulation, characterization and in vivo evaluation. J Drug Deliv Sci Technol. 2023;80:104203. doi: 10.1016/j.jddst.2023.104203.
26. Sahibzada MU, Sadiq A, Faidah HS, Khurram M, Amin MU, Haseeb A, et al. Berberine nanoparticles with enhanced in vitro bioavailability: characterization and antimicrobial activity. Drug Des Devel Ther. 2018;12:303-12. doi: 10.2147/dddt.S156123.
27. Sinha N, Singh BK, Dutta PK. Research on antibacterial screening and drug delivery using chitosan-stearic acid derivative. J Polym Mater. 2017;34:11-20.
28. Antoniraj MG, Kumar CS, Kandasamy R. Synthesis and characterization of poly (N-isopropylacrylamide)-g-carboxymethyl chitosan copolymer-based doxorubicin-loaded polymeric nanoparticles for thermoresponsive drug release. Colloid Polym Sci. 2016;294(3):527-35. doi: 10.1007/s00396-015-3804-4.
29. Sajomsang W, Gonil P, Saesoo S, Ruktanonchai UR, Srinuanchai W, Puttipipatkhachorn S. Synthesis and anticervical cancer activity of novel pH responsive micelles for oral curcumin delivery. Int J Pharm. 2014;477(1-2):261-72. doi: 10.1016/j.ijpharm.2014.10.042.
30. Rajaei A, Salarbashi D, Tafaghodi M, Sabeti Z, Sabbagh F, Rakhshani S, et al. Evaluation of antimicrobial and structural properties of thyme essential oil-loaded chitosan-capric acid and chitosan-stearic acid nanogels. J Food Qual Hazards Control. 2023;10(3):153-62. doi: 10.18502/jfqhc.10.3.13646.
31. Cojocaru V, Ranetti AE, Hinescu LG, Ionescu M, Cosmescu C, Poștoarcă AG, et al. Formulation and evaluation of in vitro release kinetics of Na3CaDTPA decorporation agent embedded in microemulsion-based gel formulation for topical delivery. Farmacia. 2015;63(5):656-64.
32. Farahani M, Moradikhah F, Shabani I, Karimi Soflou R, Seyedjafari E. Microfluidic fabrication of berberine-loaded nanoparticles for cancer treatment applications. J Drug Deliv Sci Technol. 2021;61:102134. doi: 10.1016/j.jddst.2020.102134.
33. Pund S, Borade G, Rasve G. Improvement of anti-inflammatory and anti-angiogenic activity of berberine by novel rapid dissolving nanoemulsifying technique. Phytomedicine. 2014;21(3):307-14. doi: 10.1016/j.phymed.2013.09.013.
34. Mahya S, Ai J, Shojae S, Khonakdar HA, Darbemamieh G, Shirian S. Berberine loaded chitosan nanoparticles encapsulated in polysaccharide-based hydrogel for the repair of spinal cord. Int J Biol Macromol. 2021;182:82-90. doi: 10.1016/j.ijbiomac.2021.03.106.
35. Liu Y, Xie X, Chen H, Hou X, He Y, Shen J, et al. Advances in next-generation lipid-polymer hybrid nanocarriers with emphasis on polymer-modified functional liposomes and cell-based-biomimetic nanocarriers for active ingredients and fractions from Chinese medicine delivery. Nanomedicine. 2020;29:102237. doi: 10.1016/j.nano.2020.102237.
36. Meng T, Wu J, Yi H, Liu J, Lu B, Yuan M, et al. A spermine conjugated stearic acid-g-chitosan oligosaccharide polymer with different types of amino groups for efficient p53 gene therapy. Colloids Surf B Biointerfaces. 2016;145:695-705. doi: 10.1016/j.colsurfb.2016.05.071.
37. Gan Q, Wang T, Cochrane C, McCarron P. Modulation of surface charge, particle size and morphological properties of chitosan-TPP nanoparticles intended for gene delivery. Colloids Surf B Biointerfaces. 2005;44(2-3):65-73. doi: 10.1016/j.colsurfb.2005.06.001.
38. Aibani N, Rai R, Patel P, Cuddihy G, Wasan EK. Chitosan nanoparticles at the biological interface: implications for drug delivery. Pharmaceutics. 2021;13(10):1686. doi: 10.3390/pharmaceutics13101686.
39. Thandapani G, Supriya Prasad P, Sudha PN, Sukumaran A. Size optimization and in vitro biocompatibility studies of chitosan nanoparticles. Int J Biol Macromol. 2017;104(Pt B):1794-806. doi: 10.1016/j.ijbiomac.2017.08.057.
40. Verheul RJ, Amidi M, van Steenbergen MJ, van Riet E, Jiskoot W, Hennink WE. Influence of the degree of acetylation on the enzymatic degradation and in vitro biological properties of trimethylated chitosans. Biomaterials. 2009;30(18):3129-35. doi: 10.1016/j.biomaterials.2009.03.013.
41. Tomihata K, Ikada Y. In vitro and in vivo degradation of films of chitin and its deacetylated derivatives. Biomaterials. 1997;18(7):567-75. doi: 10.1016/s0142-9612(96)00167-6.
42. Saravanabhavan SS, Bose R, Skylab S, Dharmalingam S. Fabrication of chitosan/TPP nano particles as a carrier towards the treatment of cancer. Int J Drug Deliv. 2013;5(1):35-42.
43. Yang Y, Yuan SX, Zhao LH, Wang C, Ni JS, Wang ZG, et al. Ligand-directed stearic acid grafted chitosan micelles to increase therapeutic efficacy in hepatic cancer. Mol Pharm. 2015;12(2):644-52. doi: 10.1021/mp500723k.
44. Abo El-Enin HA, Elkomy MH, Naguib IA, Ahmed MF, Alsaidan OA, Alsalahat I, et al. Lipid nanocarriers overlaid with chitosan for brain delivery of berberine via the nasal route. Pharmaceuticals (Basel). 2022;15(3):281. doi: 10.3390/ph15030281.
45. Andreani T, Cheng R, Elbadri K, Ferro C, Menezes T, Dos Santos MR, et al. Natural compounds-based nanomedicines for cancer treatment: future directions and challenges. Drug Deliv Transl Res. 2024;14(10):2845-916. doi: 10.1007/s13346-024-01649-z.
46. Sood A, Gupta A, Bharadwaj R, Ranganath P, Silverman N, Agrawal G. Biodegradable disulfide crosslinked chitosan/stearic acid nanoparticles for dual drug delivery for colorectal cancer. Carbohydr Polym. 2022;294:119833. doi: 10.1016/j.carbpol.2022.119833.
47. Yang X, Lian K, Tan Y, Zhu Y, Liu X, Zeng Y, et al. Selective uptake of chitosan polymeric micelles by circulating monocytes for enhanced tumor targeting. Carbohydr Polym. 2020;229:115435. doi: 10.1016/j.carbpol.2019.115435.
48. Hu FQ, Wu XL, Du YZ, You J, Yuan H. Cellular uptake and cytotoxicity of shell crosslinked stearic acid-grafted chitosan oligosaccharide micelles encapsulating doxorubicin. Eur J Pharm Biopharm. 2008;69(1):117-25. doi: 10.1016/j.ejpb.2007.09.018.
49. Hu FQ, Jiang XH, Huang X, Wu XL, Yuan H, Wei XH, et al. Enhanced cellular uptake of chlorine e6 mediated by stearic acid-grafted chitosan oligosaccharide micelles. J Drug Target. 2009;17(5):384-91. doi: 10.1080/10611860902894325.
50. Victorelli FD, de Oliveira Cardoso VM, Ferreira NN, Calixto GM, Fontana CR, Baltazar F, et al. Chick embryo chorioallantoic membrane as a suitable in vivo model to evaluate drug delivery systems for cancer treatment: a review. Eur J Pharm Biopharm. 2020;153:273-84. doi: 10.1016/j.ejpb.2020.06.010.
51. Zarei B, Homayouni Tabrizi M, Rahmati A. PEGylated lecithin-chitosan nanoparticle-encapsulated alpha-terpineol for in vitro anticancer effects. AAPS PharmSciTech. 2022;23(4):94. doi: 10.1208/s12249-022-02245-5.